

## ABSTRACT

YIN, MENGCHEN. Dehydrocyclization of n-Paraffins into Aromatics over Pd/C Catalyst. (Under the direction of Dr. William Roberts and Dr. Praveen Kolar).

The n-octane gas-phase dehydrocyclization activity and selectivity of Pd/C is compared with several catalysts and studied over a range of operating conditions, including: temperatures, WHSV (weight hourly space velocities), and  $H_2/n-C_8H_{18}$  molar ratios. The Pt- or Pd-supported catalysts studied include: Pd/C, Pt/C, Pt/KL, Pd/zeolite and Pt/ $Al_2O_3$ . For the conditions studied, Pd/C exhibited the best dehydrocyclization performance, including 54.4% n- $C_8H_{18}$  conversion and 31.5% aromatics yield at 500 °C,  $WHSV=2\ h^{-1}$ , and a  $H_2/n-C_8H_{18}$  molar ratio of 2. At the same conditions, Pt/C had 85.0% n- $C_8H_{18}$  conversion and a 15.6% aromatics yield; Pt/KL had 74.5% conversion and a 21.1% aromatics yield. The Pd/C catalyst had higher selectivities towards the preferred aromatic products: ethylbenzene and xylenes, whereas Pt/KL had higher selectivities towards benzene and toluene. These results are consistent with adsorbed n-octane cyclization proceeding mainly through the six-membered ring closure mechanism over the Pd/C catalyst. In addition, Pd/C was explored qualitatively with n-hexane and n-heptane as reactants and showed capability of catalyzing aromatization over n-alkanes with varying chain length.

© Copyright 2011 by Mengchen Yin

All Rights Reserved

Dehydrocyclization of n-Paraffins into Aromatics over Pd/C Catalyst

by  
Mengchen Yin

A thesis submitted to the Graduate Faculty of  
North Carolina State University  
in partial fulfillment of the  
requirements for the degree of  
Master of Science

Mechanical Engineering

Raleigh, North Carolina

2011

APPROVED BY:

---

Tiegang Fang

---

Praveen Kolar

---

William Roberts

Committee Chair

## **DEDICATION**

To my beloved family and friends!

## BIOGRAPHY

Mengchen Yin was brought to this world, without previous notice, by Cuie Liu and Wenya Yin in the early morning on April 13<sup>th</sup>, 1988 in Changsha, Hunan. His name composed Chinese character ‘dream’ and ‘morning’, was a quite poetical, even sort of feminine name. He thereupon was asked to clean lady’s room in high school just because his name appeared on the roll list confused his teacher. He was never an easy-raised boy since he was a child. He refused to eat because he didn’t know what is hungry; He loved to be an entomologist because he was the only child at home, and only had bugs to play with. After entering middle school, he was addicted in computer games and determined to be a hacker, with a quite simple reason: to cheat in the game. Soon he was restrained from any computers, and his attention was transferred to cars, which could take him far away, maybe somewhere with lots of computers. He chose Automotive Engineering as his major in a university, and then further pursued his graduate education in a new continent. He hoped he could contribute to this field someday in the future. His graduate research was a little bit deviated, he was still sticking to this little dream though.

## ACKNOWLEDGMENTS

I wish to thank all those who helped me, without them, this thesis could not have been written. They are:

Professor William Roberts, who gave me the precious opportunity to work in this Bio-fuel project and influenced me with his intellectual thought.

Professor Praveen Kolar, who cast light on the catalytic reactions, instructed and encouraged me throughout the research.

Wilson Wang, Nirajan, Abhisheka, Robert and Andrew, who guided me through the operational procedure and gave me lots of handy help, and became friends with me.

My housemate Zhuo Tan and Xiaofan He, who gave me countless care and warm.

My family and all my friends, who always stand behind me.

And God, who made all this possible.

## TABLE OF CONTENTS

<b>LIST OF TABLES.....</b>	<b>vi</b>
<b>LIST OF FIGURES.....</b>	<b>vii</b>
<b>Chapter 1 Introduction .....</b>	<b>1</b>
<b>Chapter 2 Experimental.....</b>	<b>8</b>
2.1 Catalyst preparation .....	8
2.2 Catalyst characterization .....	9
2.3 Dehydrocyclization reaction .....	9
2.4 Analytical methods.....	10
<b>Chapter 3 Results and discussion .....</b>	<b>23</b>
3.1 Catalytic performance of Pd/C .....	23
3.2 Comparisons between different catalysts .....	32
3.3 Comparisons between different feedstock.....	38
<b>Chapter 4 Conclusions .....</b>	<b>40</b>
<b>REFERENCES .....</b>	<b>42</b>

**LIST OF TABLES**

Table 1.1 A comparison of the freeze point and flash point of paraffins and aromatics with JP-8 .....	3
Table 2.1 Different concentration of components and their corresponding area counts .....	13
Table 2.2 Peak area and certificated concentration of each component .....	19
Table 2.3 The peak areas for pure standards .....	19
Table 2.4 Comparison of evaluated concentration with the theoretical concentration .....	20
Table 3.1 Conversion and total aromatics selectivity of n-octane dehydrocyclization over Pd/C at various WHSV .....	28
Table 3.2 Conversion and total aromatics selectivity of n-octane dehydrocyclization over Pd/C at various hydrogen/C8 molar ratios .....	30
Table 3.3 Dehydrocyclization of n-octane over different Pd, Pt catalysts .....	32

**LIST OF FIGURES**

Figure 1.1 Red Wolf Refining process .....	5
Figure 2.1 A general schematic view of reactor setup.....	10
Figure 2.2 Separate points for benzene with calibration curve fitted by linear regression .....	14
Figure 2.3 Average points for benzene with calibration curve fitted by linear regression .....	14
Figure 2.4 Separate points for toluene and calibration curve fitted by linear regression .....	15
Figure 2.5 Average points for toluene and calibration curve fitted by linear regressio .....	15
Figure 2.6 Concentration of benzene and corresponding area counts with calibration curve fitted by B spline .....	16
Figure 2.7 Concentration of toluene and corresponding area counts with calibration curve fitted by B spline .....	17
Figure 3.1 Effect of temperature on conversion of n-octane over Pd/C, yield of total aromatics and selectivity .....	24
Figure 3.2 Effect of reaction temperature on aromatics selectivity during conversion of n- Octane over Pd/C .....	27
Figure 3.3 Effect of reaction time on total conversion, aromatics selectivity and yield of n- octane over Pd/C.....	34
Figure 3.4 Effect of reaction time on total conversion, aromatics selectivity and yield of n- octane over Pt/KL.....	35

Figure 3.5 Effect of reaction time on total conversion, aromatics selectivity and yield of n-octane over Pt/C .....	36
Figure 3.6 GC/FID chromatograms from aromatization over Pd/C .....	39

# Chapter 1 Introduction

Increased global consumption of liquid transportation fuels as well as growing concerns of anthropogenic CO<sub>2</sub> have led to a greater interest in biofuels. To-date, processes that produce hydrocarbon-based biofuels lack a step to produce aromatics (i.e., hydrogenation, Fischer-Tropsch synthesis of gasified biomass, decarboxylation; excluding pyrolysis of lignin). Aromatics increase the octane rating of bio-gasoline or provide solvent characteristics in Bio-SPK (bio-derived synthetic paraffinic kerosene). The nitrile seals in an aircraft fuel system require a liquid (jet) fuel with a minimum aromatic content of approximately 8% to swell [1]; if an unblended paraffinic kerosene (e.g., Bio-SPK) were to be used in an aircraft, leakages would occur at the site of the nitrile seal. Currently, Bio-SPK fuels are blended on a 50:50 basis with aromatic-rich and petroleum-derived jet fuel in order to satisfy the aromatic content requirement. Dehydrocyclization of the paraffins in Bio-SPK is a method for producing a drop-in "neat" bio-jet fuel that is completely renewable; in addition, the H<sub>2</sub> produced in this reaction further decouples biofuel processes from fossil fuels (i.e., H<sub>2</sub> is mostly produced from steam reforming or partial oxidation of CH<sub>4</sub>).

Aromatics are already found in petroleum-derived fuels, though their proportions in transportation fuels are controlled. Benzene is known as a chemical carcinogen that can be discharged in the exhaust gas as an unburned hydro-carbon [2] or vaporize during the fuel storage and handling. A benzene constraint of 0.62% by volume on both conventional and reformulated gasolines has been imposed in the U.S. [3]. However, the total aromatics have constraints of 42% and 48% maximum for regular and premium gasolines, respectively. The

higher tolerance for aromatics in premium gasoline is indicative of the positive correlation between aromatics and octane rating.

Jet fuel ASTM guidelines require a low freezing point (Jet-A1, JP-8, JP-5:  $<-47\text{ }^{\circ}\text{C}$ ; Jet-A:  $<-40\text{ }^{\circ}\text{C}$ ) and a moderate flash point (JP-8, Jet-A, Jet-A1:  $>38\text{ }^{\circ}\text{C}$ ; JP-5:  $>60\text{ }^{\circ}\text{C}$ ) to meet specification. Longer chained (C16+) molecules have high flash points and high freeze points; shorter chained hydrocarbons (C5-C9) have low flash points and low freeze points. A middle distillate range of C10-C14 hydrocarbons provides a balance to where both a low freeze point (due to a significant contribution of iso-paraffins) and moderate flash point are achievable [1]. The values for various molecules of interest in this study are given in Table 1. For the given molecules this table shows that m-xylene is the closest to meeting the JP-8 requirement for both the freeze point and flash point; in addition, it shows that the site-location of the substitution does affect the intrinsic properties of the molecule. While none of the molecules meets the JP-8 specification by itself, it is clear that benzene, which has both a high freezing point and low flash point, would be a poor candidate for a JP-8 fuel blend [4]. An 8% by volume blend of m-xylene or ethylbenzene into a Bio-SPK would have a lesser adverse impact on the flash point and freeze point of the fuel relative to benzene or toluene.

Table 1.1 A comparison of the freeze point and flash point of paraffins and aromatics with JP-8 [5-6]

Molecule or fuel	Freeze point	Flash point
JP-8	<-47 °C	>38 °C
n-hexane	-95 °C	-23 °C
n-octane	-57 °C	13 °C
benzene	5.5 °C	-11 °C
toluene	-93 °C	4 °C
o-xylene	-25 °C	17 °C
m-xylene	-48 °C	25 °C
p-xylene	13 °C	25 °C
ethylbenzene	-95 °C	15 °C

Red Wolf refining technology is a thermal-chemical catalytic process (Fig. 1.1) that makes fuel from crops such as jatropha, camelina, soy, canola, palm, yellow grease (chicken fat), and hog fat. It converts fatty oils into diesel, jet and gasoline fuel via a four-step process, which are [7]:

1) Hydrolysis

Feedstock (including fats, oils and lipids) are heated under pressure to react with water and separate the fatty acid chains from the glycerol backbone. This is accomplished by separately pumping steam and (the fat-containing) oil at moderate temperature and pressures into a Colgate-Emery reactor.

## 2) Deoxygenation

This step, also known as decarboxylation, takes the free fatty acid from the hydrolysis reactor and removes any degrees of unsaturation of the fatty free acid. The product of this reaction is a straight-chained hydrocarbon which is then reformed into the desired fuel.

## 3) Reforming to Green Diesel, Bio-jet Fuel or Bio-gasoline

There are two parts to this step. Isomerization and cracking products are designed to have a lower freezing point than the deoxygenated free fatty acid. This is followed by dehydrocyclization (also known as aromatization) to convert and create the final fuel products into aromatic compounds, which typically display enhanced chemical stability. These aromatics formed are necessary to meet specifications for jet fuel and are also a common component in gasoline to raise the octane rating.

## 4) Combustion

The parallel combustion of the glycerol byproduct as previously stated results in it serving as the thermal energy source for all three previous steps. This step increases the energy efficiency of the process as well as minimizes waste streams.

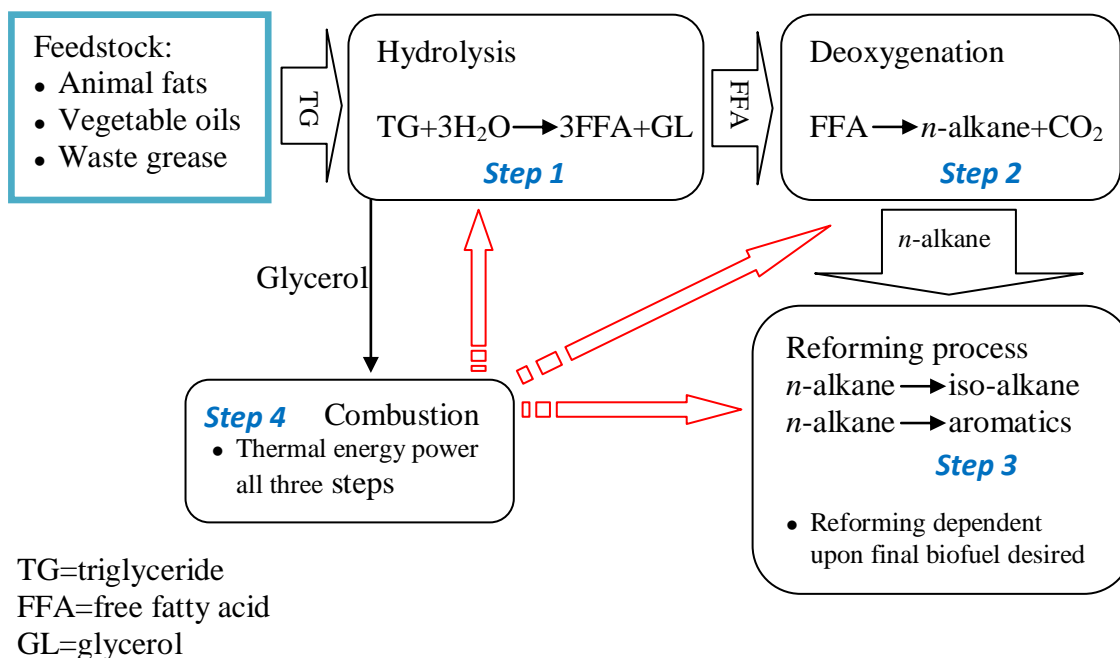


Figure 1.1 Red Wolf Refining process

As mentioned earlier, dehydrocyclization is a process that involves both dehydrogenation and cyclization. There are three well-known catalysts for dehydrocyclization: Pt/ZSM-5, Pt/Al<sub>2</sub>O<sub>3</sub> and Pt/KL. Catalyst formulations with high selectivities toward alkyl-substituted benzenes from *n*-paraffins and iso-paraffins are of great interest for jet fuel and gasoline applications.

Pt is well known to exhibit dehydrocyclization activity [8]. Davis and Venuto investigated Pt/Al<sub>2</sub>O<sub>3</sub> that was known for its effect in the naphtha reforming process in the 1950s using a Vycor glass reaction tube coupled with a preheater section [9]. They used Al<sub>2</sub>O<sub>3</sub>-K, Al<sub>2</sub>O<sub>3</sub>-Li, Pt-Al<sub>2</sub>O<sub>3</sub>-K, Pt-Al<sub>2</sub>O<sub>3</sub>-Li, and Pt-SiO<sub>2</sub> for aromatization to compare between bifunctional and monofunctional catalysts for dehydrocyclization activity and selectivity. Products measured from the aromatization of 10 different C8-C9 alkanes

confirmed that direct six-membered ring closure was the preferred mechanism for aromatization. A Pt/Al<sub>2</sub>O<sub>3</sub> study conducted by Rangel et al. using n-octane as feedstock reported selectivity of 1.3% benzene, 3.0% toluene, 26% m-xylene, 19.9% o-xylene, 8.6% p-xylene and 10.3% ethylbenzene and total conversion of 87.6% after 1 h on stream [10]. After preparation with the wet impregnation method using  $\gamma$ -Al<sub>2</sub>O<sub>3</sub>, the experiments were conducted at 500 °C, 19 H<sub>2</sub>/n-octane molar ratio, and atmospheric pressure. The behavior of Pt/Al<sub>2</sub>O<sub>3</sub> with feeding n-octane was also studied by Davis and co-workers [11]. They reported 33.8% of conversion and selectivity of 25.6% ethylbenzene, 31.4% o-xylene, 29.3% m-xylene, and 13.7% p-xylene after 1 h on stream, with catalyst synthesized by incipient wetness technique using commercial alumina from United Catalysts Inc., and experiments were conducted at 482 °C, 8 H<sub>2</sub>/n-octane molar ratio and atmospheric pressure. In other studies, metal clusters of Pt incorporated into the channels of zeolite L have been found to catalyze the dehydrocyclization of hexane and heptane with a high activity and selectivity [12-14]. Specifically, Bernard [13] discovered that platinum supported on the K<sup>+</sup>-exchanged form of zeolite L (Pt/KL) was more active than other previous known catalysts in this reaction under experiments conditions: reaction temperature=750K, H<sub>2</sub>/n-alkane molar ratio=6 and atmospheric pressure. In addition, a study of aromatization of n-octane over Pt/KL reported the product distribution was 37.7% of conversion rate and selectivity to benzene, toluene, ethylbenzene, m- and p- xylene and o-xylene were 27.7%, 28.3%, 6.5%, 1.4% and 3.0% after 10 h on stream under reaction conditions: 500 °C, H<sub>2</sub>/n-C<sub>8</sub> 6:1 molar ratio, WHSV 5 h<sup>-1</sup> [15]. From a review on the aromatization of liquefied petroleum gas (LPG) to BTX (benzene, toluene, and xylenes), it was observed that commonly zeolites with

mordenite framework inverted (MFI) pore structure were often chosen as support for Pt to catalyze aromatization, known for its resistance to coking [16].

Pd, another group VIII metal, has been demonstrated to catalyze the hydrogenation and dehydrogenation reactions [17]. This has been shown in the literature for the deoxygenation and decarboxylation reactions [18-19] and C-C forming process like the Suzuki coupling, Heck coupling and Stille reactions [20]. While Pd has not received much attention in dehydrocyclization studies, there is rare application of such metal as catalysts of dehydrocyclization. Different catalysts were used for comparison. Pt/Al<sub>2</sub>O<sub>3</sub> and Pt/KL were selected because they are common aromatization catalysts, other catalyst-support systems, such as Pd/zeolite and Pt/C were studied to decouple the metal and support effects. C<sub>6</sub> to C<sub>8</sub> alkanes also were tested on Pd/C, because they are the expected products from Redwolf's decarboxylation process that prior to the aromatization process. Specific objectives were to (1) determine the catalysts behavior over a range of operating experimental conditions with temperature from 400 °C to 600 °C, WHSV from 0.8 to infinity and hydrogen to hydrocarbon molar ratio from 0 to 6; (2) evaluate the efficiency and longevity of Pd/C relative to such as Pd/Zeolite, Pt/Al<sub>2</sub>O<sub>3</sub>, Pt/C and Pt/KL catalysts; (3) test the adaptability of Pd/C for different alkanes including n-hexane, n-heptane and n-octane, which are expected products from the Red Wolf Refining<sup>TM</sup> decarboxylation process that is prior to the aromatization process.

## Chapter 2 Experimental

### 2.1 Catalyst preparation

Five catalysts, Pd/C, Pd/Zeolite, Pt/Al<sub>2</sub>O<sub>3</sub>, Pt/C and Pt/KL, were tested for the dehydrocyclization of n-octane. Three of them were acquired as commercial catalysts; 5 wt% Pd/C (E117 PB/W) catalyst was purchased from Evonik Industries, which had been pre-reduced in the manufacturing process, Pt/Al<sub>2</sub>O<sub>3</sub> catalyst with 5 wt% Pt was purchased from Shaanxi Kaida Chemical Engineering Co., Ltd, and 1% Pd/Zeolite (Zeolyst 870) was purchased from Zeolyst international. Pt/KL catalyst was prepared with 1 wt% Pt, and the K-L support was obtained from the Tosoh Corporation (HSZ 500KOA). The support was loaded with 1% Pt (wt. basis) using incipient wetness impregnation methods. The catalyst was dried overnight at 105 °C, and then calcined at 350 °C for 4 h, using a ramp rate of 2 °C/min from room temperature. The catalyst was synthesized via incipient wetness method. First the precursor solution was prepared by dissolving chloroplatinic acid hexahydrate (Fisher Scientific) in deionized water. Coconut shell derived granular activated carbon (Fisher Scientific) was added to the solution and the salt solution was allowed to adsorb on carbon surface for eight hours. The catalyst was dried overnight at 105 °C and calcined at 300 °C for 2 h.

Pt/Al<sub>2</sub>O<sub>3</sub> was reduced in-situ at 500 °C and 101 kPa for 2 h with hydrogen flow at 35 sccm prior to the n-octane feeding, according to the method of Rangel et al. [10].

Pt/C was reduced under hydrogen flow and heated at 350 °C for 2 h, following the same procedure as the study Román-Martínez et al. conducted [21]. The Pt/C was

constructed in the form of a large pellet; it was further grinded into a smaller powder. This was done because hydrogenolysis and cracking become significant reaction pathways with large Pt particles relative to the rates of these two reactions with very small Pt particles [22]. The particle size was still large relative to the commercial variety after grinding.

For the pretreatment of the Pt/KL, the catalyst was reduced in the reactor at 500 °C and 101 kPa for 2 h with hydrogen flow rate of 55 sccm, which was the methods Siriporn et al. used [15].

Pd/Zeolite was specially adopted as an analog to Pt/KL. There is no prior work being done with this catalyst in aromatization, therefore it was pretreated at the same procedure as was Pt/KL

## 2.2 Catalyst characterization

The surface area tests were conducted by the BET N<sub>2</sub> adsorption method; a Gemini VII 2390 Surface Area Analyzer was used to carry out the test. The fresh Pd/C was measured to have a 35 μm median particle size (size wise 90 % of the fresh catalyst was under 110 microns and 10% of the catalyst was under 10 microns) and Pd was of uniform distribution. The BET surface area for Pd/C was 809 m<sup>2</sup>/g and with total pore volume at 0.5009 P/P<sub>0</sub> to be 0.43cm<sup>3</sup>/g. Pulse CO chemisorptions of the Pd showed dispersion around 29% [18].

## 2.3 Dehydrocyclization reaction

Dehydrocyclization was studied as a catalytic gas phase reaction carried out in a custom made continuous tubular reactor, which consisted of two separate 2.54 cm (OD) steel tubes (the vaporizer and the reactor) that have been welded together via a 0.635 cm (OD)

tube. The feed and gas flow inlets are located at the end of the vaporizer section, and an outlet has been connected to the reactor end. Both tubes were coated with coiling wires and insulation cover, and were heated by two induction ovens and controlled by two temperature controllers. Normally, the vaporizer temperature was set to be around 30 °C higher than the boiling point of the reactant (e.g. vaporizer temperature of n-octane feeding reactions was set at 160 °C). Gas flow rate and composition were controlled by mass flow controllers (Brooks 5850E series) at the upstream of the reactor and a HPLC pump (Waters Millipore 510) injected reactants into the reactor. The reactor was set horizontally. The catalyst was retained and plugged by glass wool. From the end of the reactor, a 5 cm transfer line sent the product to the condenser with coolant (anti-freeze ethylene glycol) of -1 °C flowing through it. As the gas phase product passed, it condensed into liquid and was collected in a flask; the waste gas was exhausted through the gas exit line.

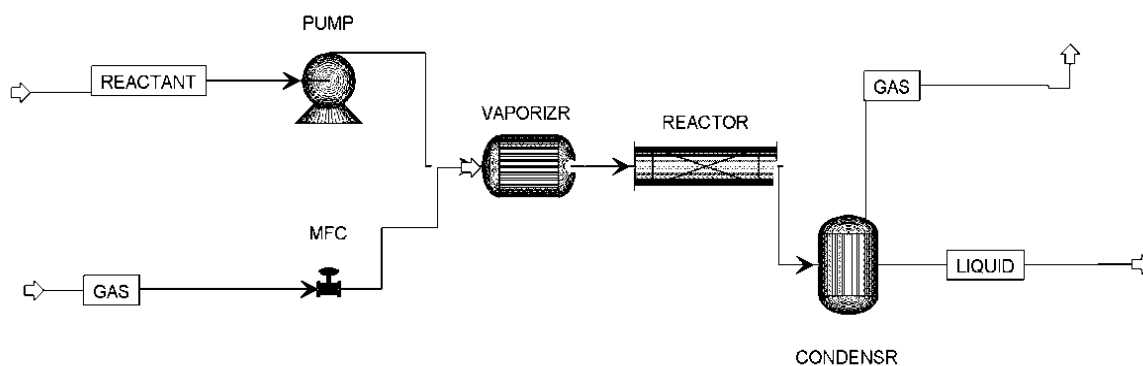


Figure 2.1 A general schematic view of reactor setup

## 2.4 Analytical methods

A gas chromatograph with mass spectrometry (GC-MS) was used for the identification and quantification of products. Measurements were performed with an Agilent 7890A gas chromatograph coupled to an Agilent 5975C inert XL mass spectrometry

detector. The sample injections were conducted by an Agilent 7693 autosampler with G4513A injector. The products were separated by an Agilent 190915-433 capillary column (30m  $\times$  250  $\mu$ m  $\times$  0.25  $\mu$ m). The temperature program was as follows: initial T=70  $^{\circ}$ C, then heated up with 2  $^{\circ}$ C/min to 100  $^{\circ}$ C for 5 min. Injection was in split mode at 240  $^{\circ}$ C with split ratio as 150:1, split flow was 600 ml/min of helium (purity $\geq$ 99.996%). Mass spectra were recorded at scan range 80-250 m/z.

A gas chromatograph (GC; HP 5890 Series II) equipped with flame ionization detector (FID) and a capillary column (Supelco Petrocol DH, 100 m  $\times$  0.25 mm  $\times$  0.5  $\mu$ m) was also used for quantification of products. The GC was operated under the following conditions: 1 min hold at 50  $^{\circ}$ C, 5  $^{\circ}$ C/min ramp to 180  $^{\circ}$ C, then 2  $^{\circ}$ C/min ramp to 220  $^{\circ}$ C and hold for 5 min, 15  $^{\circ}$ C/min ramp to 280  $^{\circ}$ C and hold for 5 min. The injection and detector were both set at 220  $^{\circ}$ C. An HP 7673A auto-sampler was used for injection. The split ratio was 100:1 with flow rate at 103ml/min of helium (purity $\geq$ 99.996%).

GC-MS was used to identify the components of product; the identification was based on the match with standard mass spectra available in the GC-MS library database [23]. For the quantification of the products, calibration curves were used to determine the concentration of a substance in an unknown sample by comparing the unknown to a set of standard samples of known concentration. Both GC-MS and GC-FID were adopted to make these curves for comparison.

GC-MS was used to create calibration curves for each component based on the concentration and the corresponding area. The calibration curve for benzene and toluene was made as the following procedure: Five different concentrations of benzene and toluene were

chosen for drawing the calibration curves, they were 0ppm, 1,000 ppm, 7,500ppm, 15,000ppm, and 30,000ppm. These standards were self-made ones with n-hexane as solvent. For each concentration, 3 samples were prepared in order to verify the repeatability (Table 1). Plot the known concentrations on the x-axis and the corresponding area-counts obtained from the GC-MS on the y-axis. A line of best-fit was applied to the data points. These curves were fitted by linear regression as first order linear equations:  $y = 294.09x + 634501$  ( $R^2=0.9595$ ) for the curve of benzene and  $y = 462.99x + 263289$  ( $R^2= 0.9864$ ) for the curve of toluene. Ideally, an approximate straight line with close determination coefficient ( $R^2$  close to 1) was expected to get from small concentration region. The diagrams of the calibration curves according to Table 2.1 were plotted afterward.

Table 2.1 Different concentration of components and their corresponding area counts

component	concentration (ppm)	corresponding area	component	concentration (ppm)	corresponding area
Benzene	0	0	Toluene	0	0
	0	0		0	0
	0	0		0	0
	1000	723915		1000	564312
	1000	1053194		1000	304038
	1000	1078318		1000	624405
	7500	3144852		7500	3902852
	7500	3245518		7500	4008821
	7500	2381598		7500	3634418
	15000	6168968		15000	7937681
	15000	6317399		15000	7771272
	15000	5946189		15000	8313037
	30000	8930630		30000	14419852
	30000	9217769		30000	12510684
	30000	8510261		30000	14267536

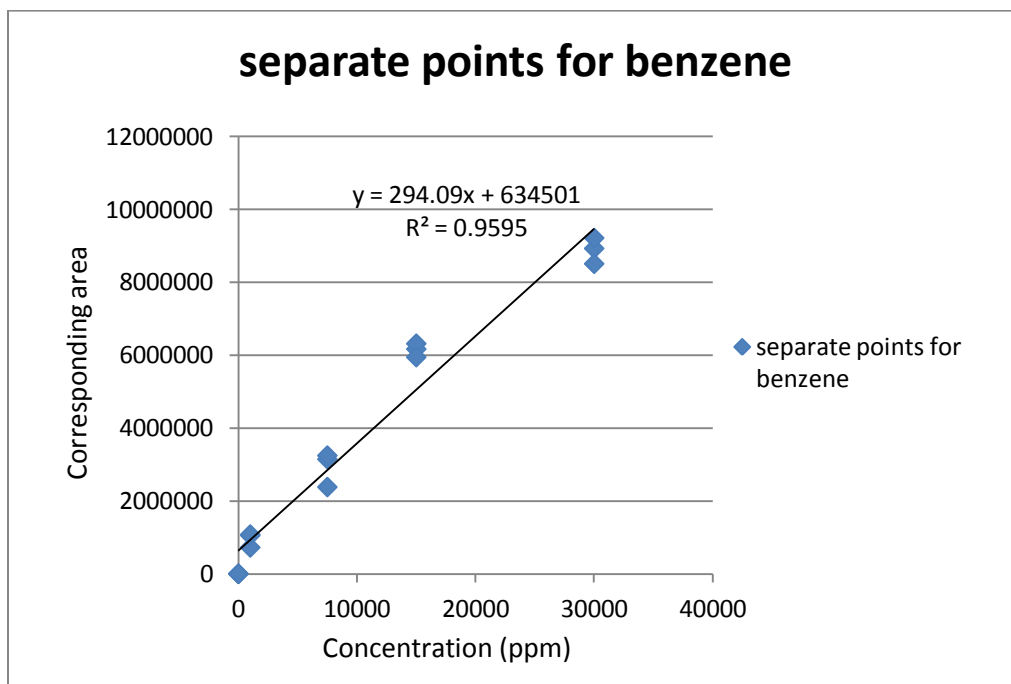


Figure 2.2 Separate points for benzene with calibration curve fitted by linear regression

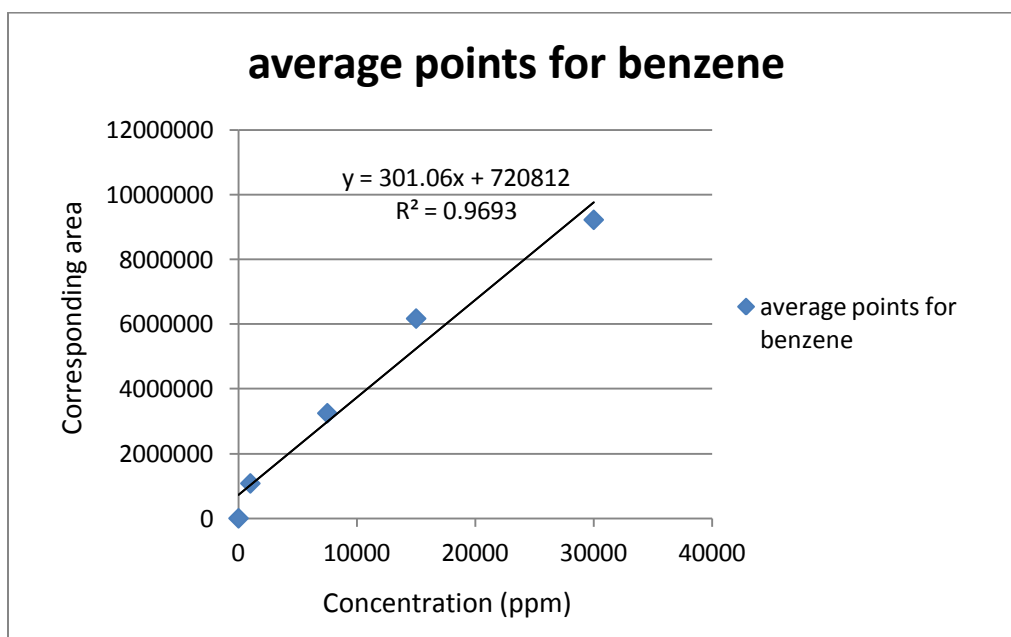


Figure 2.3 Average points for benzene with calibration curve fitted by linear regression

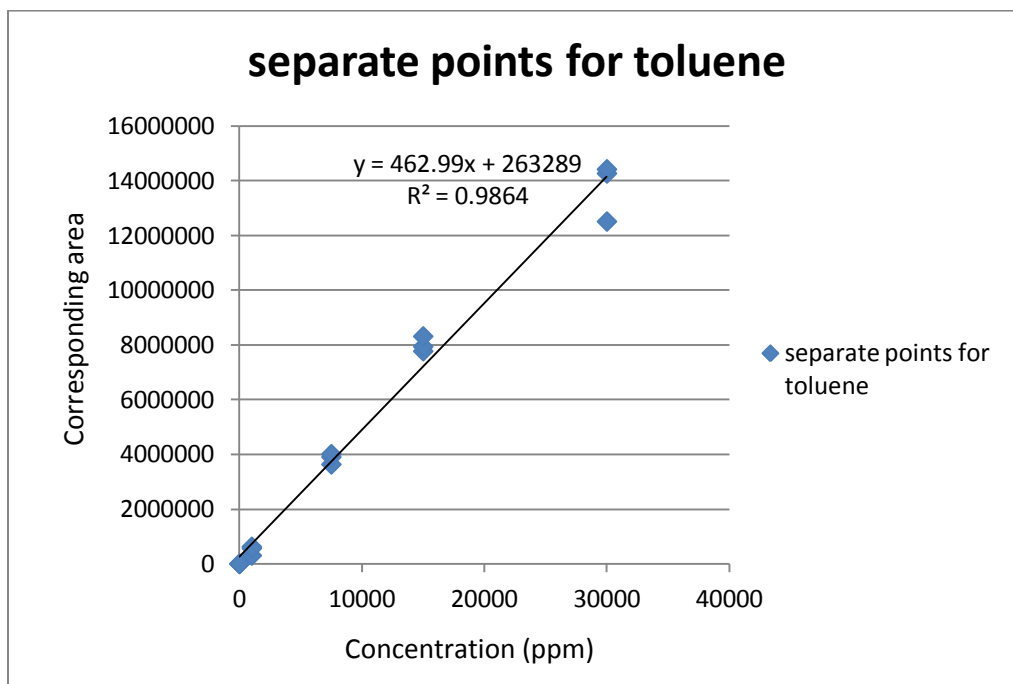


Figure 2.4 Separate points for toluene and calibration curve fitted by linear regression

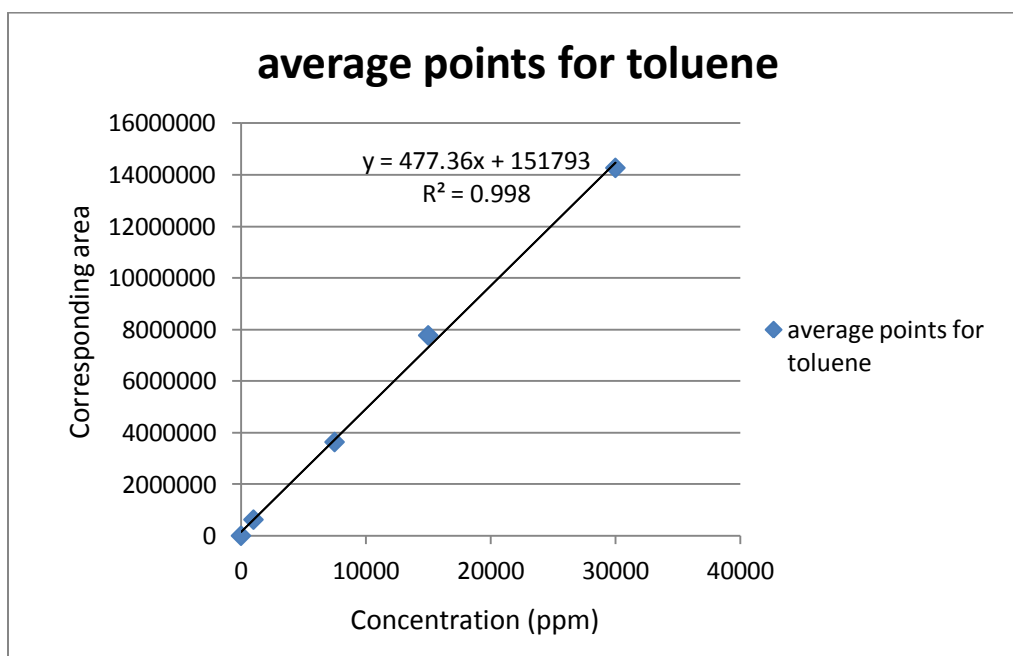


Figure 2.5 Average points for toluene and calibration curve fitted by linear regression

However, with higher concentration to be considered, the calibration curves were not proximate linear any more. Adding two other concentration points of 500,000 PPM and 1,000,000 PPM into the calibration curves with the case of benzene and toluene, the calibration curves became that shown in Fig. 2.5 and Fig. 2.6.

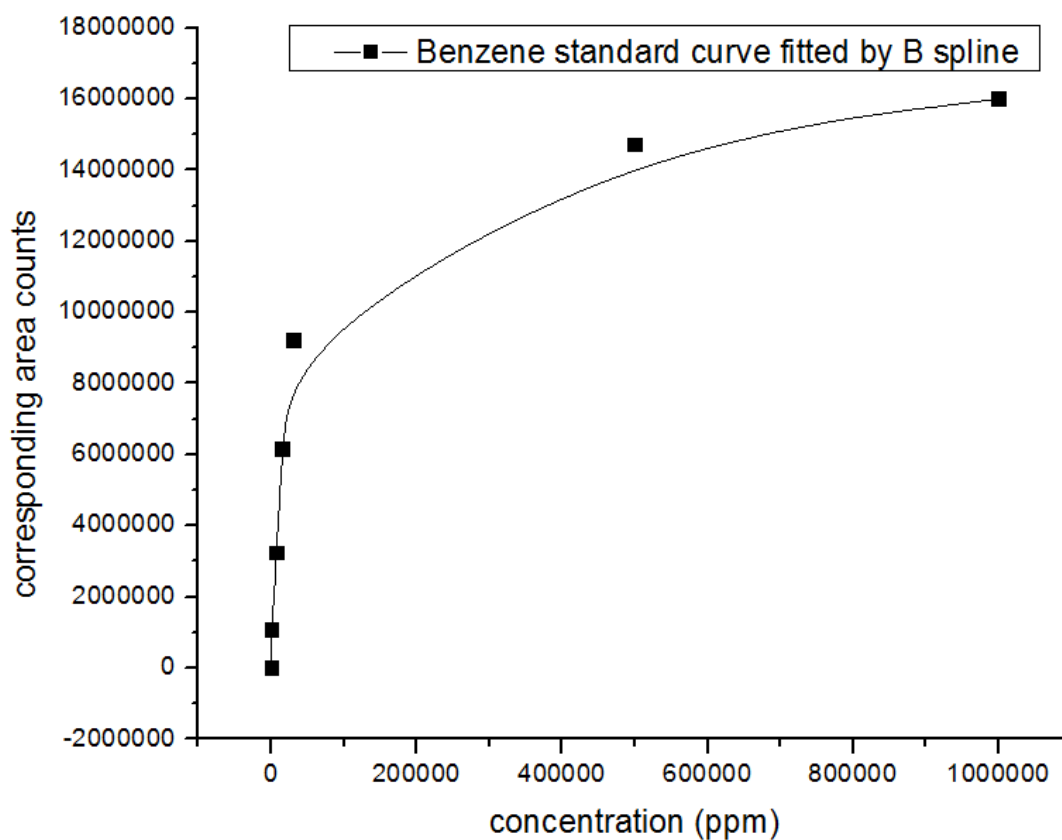


Figure 2.6 Concentration of benzene and corresponding area counts with calibration curve fitted by B spline

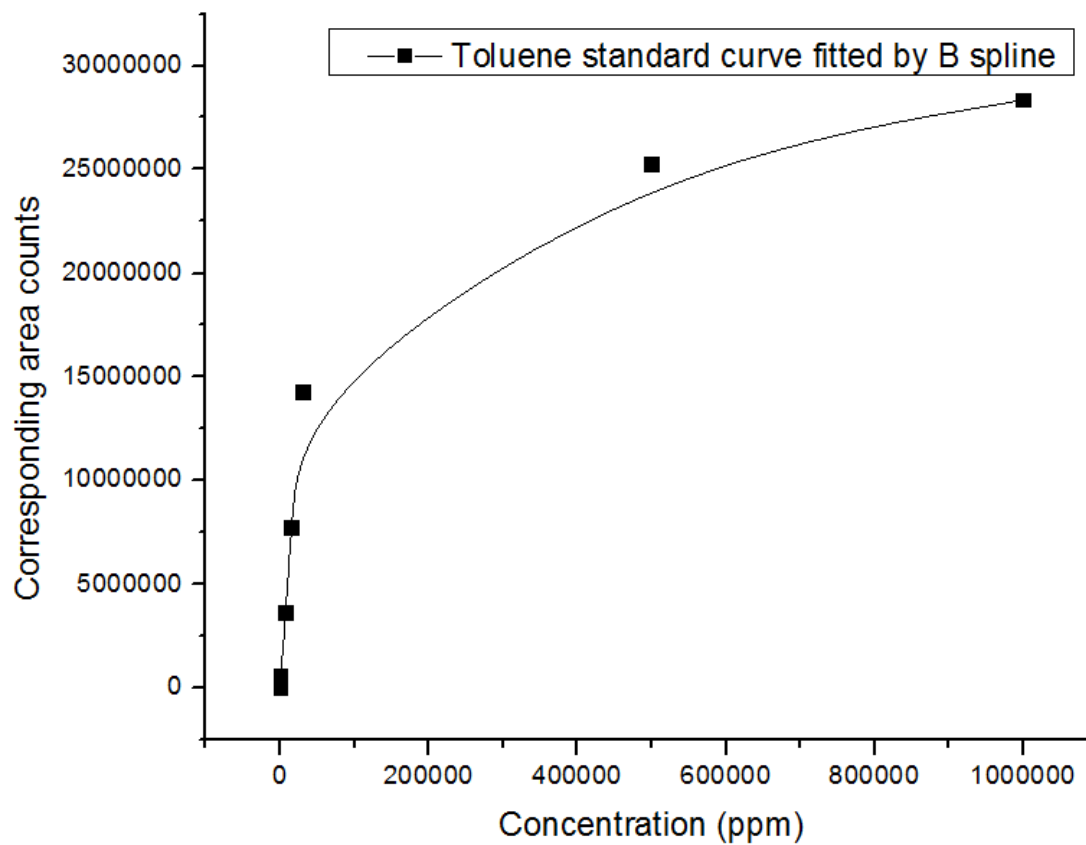


Figure 2.7 Concentration of toluene and corresponding area counts with calibration curve fitted by B spline

For those calibration curves with determination coefficient  $R^2$  equal or greater than 0.95, the assumed linearity was considered accurate enough to be used for quantification. However, with the concentration greater than 30,000, the determination coefficients of benzene and toluene were dropped out of this accurate range rapidly. Therefore, GC-MS can only be applied for quantification in a very limited range.

FID has a remarkable property that it essentially monitors and integrates carbon atoms in gaseous hydrocarbon mixtures in such an effective way irrespective of their molecular genesis. In all cases, the total ion formation rate in the flame is monitored using two electrodes, one generally the burner itself, and operated in a saturation voltage mode that ensures a withdrawal of all flame charge as it is formed. On adding traces of organic vapors to the fuel stream, great monitoring sensitivity is noted that is linear with the concentration of the additive over a wide dynamic range. Additionally, and unexpectedly, the signal to a good approximation was seen to be linearly proportional to the number of carbon atoms in the organic molecule and displayed insensitivity to its structure [24]. With this linearity characteristic, a calibration curve can be made upon only two given points. To verify this point, several experiments were conducted. A standard (Accustandard ASM-027) was purchased to make calibration curves, which contains benzene (2.0 mg/ml), Ethylbenzene (2.0 mg/ml), m-xylene (0.666 mg/ml), o-xylene (0.666 mg/ml), p-xylene (0.666 mg/ml), and toluene (2.0 mg/ml) with MeOH as solvent. The calibration curves made by GC-FID were based on the concentration and peak area. The standard was run twice by the GC-FID to examine the repeatability. The peak areas of these components, deviation between runs, average peak area and certificated concentration were listed in Table 2.2.

Table 2.2 Peak area and certificated concentration of each component

Component	Peak area of two runs		Deviation	Average peak area	Certified concentration (ppm)
Benzene	50156.3	48367.4	3.70%	49261.85	2001
Toluene	53634.5	51784.2	3.57%	52709.35	2000
Ethylbenzene	56688.2	55070.5	2.94%	55879.35	2000
P -, m-xylene*	37830.4	36478.9	3.7%	37154.65	1337
O-xylene	19336.4	18702.4	3.39%	19019.4	669

\* P-xylene and m-xylene cannot be separate by this column, the peak area was the sum of them.

Benzene (purity $\geq$ 99.9%), toluene (purity $\geq$ 99.5%), ethylbenzene (purity $\geq$ 99%), p-xylene (purity $\geq$ 99%), m-xylene (purity $\geq$ 99%), o-xylene (purity $\geq$ 99%) that purchased from Alfa Aesar company were used as pure standards to verify the linearity of calibration curves made by GC-FID. Each of these pure standards was run twice and the results had been tabulated in Table 2.3.

Table 2.3 The peak areas for pure standards

	Peak area of two runs		deviation	Average peak area
Benzene	25567248	24984574	2.33%	25275911
Toluene	27115794	26702770	1.55%	26909282
Ethylbenzene	29268356	28478108	2.77%	28873232
p-, m-xylene*	56545416	57486920	-1.64%	57016168
o-xylene	28672838	28383556	1.02%	28528197

\* P-xylene and m-xylene cannot be separate by this column, the peak area was the sum of them.

If the calibration curves made by GC-FID were highly linear,

$$\frac{\text{The average peak area of each pure standards}}{\text{The average peak area of each components withing the compound standard}} \times \text{certified concentration} \approx 1 = 1000000 \text{PPM} \quad \text{Eq.1}$$

The evaluated concentration based on the calibration curves made by GC-FID results was compared to the ideal concentration of the pure standards in the Table 2.4, the deviation was also calculated.

Table 2.4 Comparison of evaluated concentration with the theoretical concentration

	Evaluated concentration (ppm)	Theoretical concentration (ppm)	Deviation
Benzene	1026699	1000000	2.67%
Toluene	1021044	1000000	2.10%
Ethylbenzene	1033413	1000000	3.34%
p-, m-xylene*	2051711	2000000	2.59%
o-xylene	1003468	1000000	0.35%

\* P-xylene and m-xylene cannot be separate by this column, the peak area was the sum of them.

This result demonstrated not only the linearity of calibration curve over a significant range of concentration made by GC-FID, but also its repeatability and stability.

Use the equation below to get concentrations of each interest components in a target sample:

Concentration of each component in the product =

$$\frac{\text{The peak area of each component in the product}}{\text{The average peak area of each component in the compound standard}} \times \text{certified concentration} \quad \text{Eq.2}$$

The present work was gas-phase aromatization, with a very small reactant feed rate. Both the reactant and product were small in amount; therefore it was neither convenient nor accurate to measure them in volume. Quantification was concerning about concentration, which was related closely to volume, so density and mass was used for calculating volume.

For aromatization of n-octane over Pd/C, benzene, toluene, ethylbenzene, p-xylene, m-xylene and o-xylene are the main components in the product mixture, its density could be evaluated after knowing the concentration of each component.

$$\text{Mixture density} = \frac{\sum \text{Density of each component} \times \text{concentration of each component}}{\text{Sum of concentration of each component}} \quad \text{Eq. 3}$$

In this study, catalyst performances were compared with conversion, aromatics selectivity and aromatics yield, which are expressed in weight basis in Eq. 1-3:

$$\text{Conversion (wt\%)} = \frac{(\text{weight of } n\text{-alkane})_{\text{inlet}} - (\text{weight of } n\text{-alkane})_{\text{outlet}}}{(\text{weight of } n\text{-alkane})_{\text{inlet}}} \times 100 \quad \text{Eq. 4}$$

Product selectivity (wt%) =

$$\frac{\text{weight of each product}}{(\text{weight of } n\text{-alkane})_{\text{inlet}} - (\text{weight of } n\text{-alkane})_{\text{outlet}}} \times 100 \quad \text{Eq. 5}$$

$$\text{Product yield (wt\%)} = \frac{\text{weight of each product}}{(\text{weight of } n\text{-alkane})_{\text{inlet}}} \times 100 \quad \text{Eq. 6}$$

With knowing the how much reactant was consumed and how much reactant was feed, the conversion equation can be written in another form:

$$\text{Conversion (wt\%)} = \frac{\text{reactant consumed}}{\text{reactant fed}}$$

$$1 - \frac{\text{concentration of reactant in the product} \times \text{mass} \div \text{mixture density}}{\text{concentration of original reactant} \times \text{volume of reactant fed}} \quad \text{Eq. 7}$$

In the same principle, the product yield can be written as:

$$\text{Product yield (wt\%)} = \frac{\text{concentration of each component in the product} \times \text{mass} \div \text{mixture density}}{\text{concentration of original reactant} \times \text{volume of reactant fed}} \times 100 \quad \text{Eq. 8}$$

And product selectivity can simply write according to its relationship with conversion and product yield.

$$\text{Product selectivity (wt\%)} = \frac{\text{product yield}}{\text{conversion}} \quad \text{Eq. 9}$$

Total aromatics selectivity and yield were defined as the sum of the selectivity and yield of all aromatics respectively.

## Chapter 3 Results and discussion

### 3.1 Catalytic performance of Pd/C

A series of reactions were conducted with n-octane (Alfa Aesar, purity $\geq$ 98%) as feedstock and hydrogen as carrier gas. The influence of various temperatures, WHSV and hydrogen/n-octane molar ratios over conversion, selectivity, and yield was explored.

Temperature dependence of the total conversion of n-octane and the selectivity to aromatics is shown in Fig. 3.1.

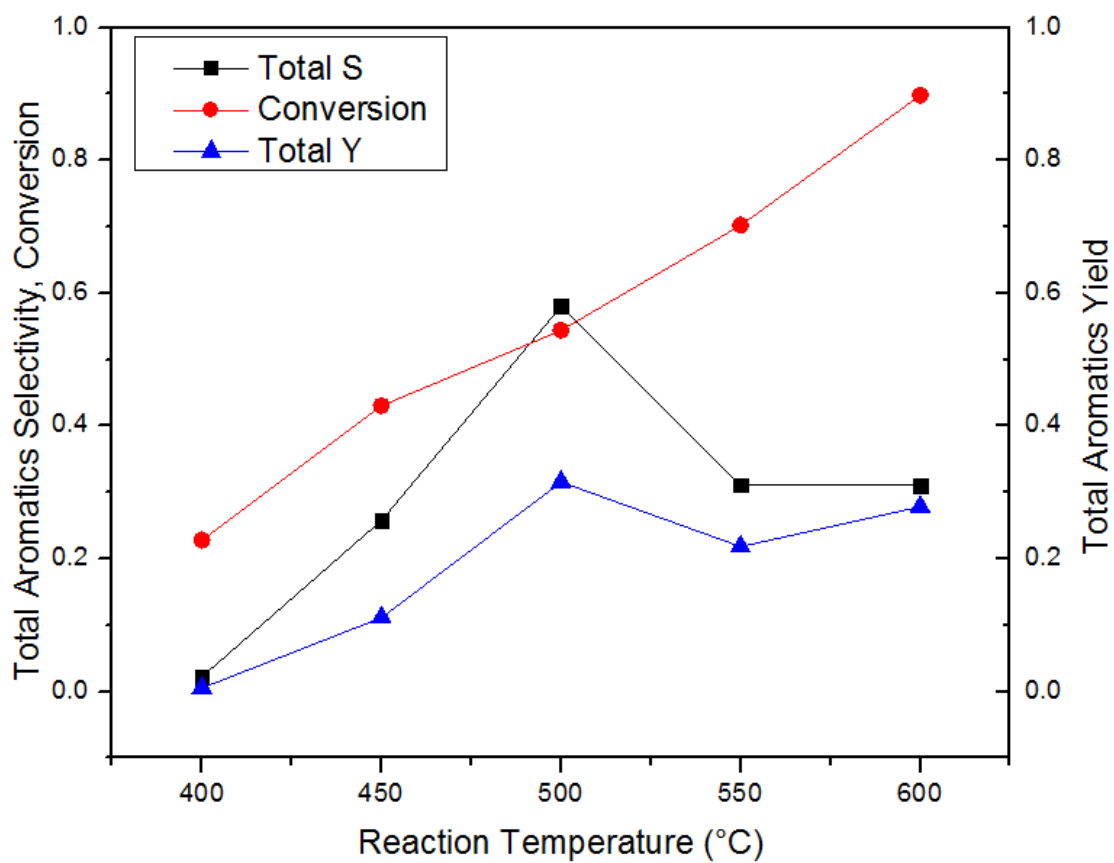


Figure 3.1 Effect of temperature on conversion of n-octane over Pd/C, yield of total aromatics and selectivity

Reaction conditions: P=100 kPa, WHSV=2 h<sup>-1</sup>, H<sub>2</sub>/n-C8 molar ratio= 2, 30 min on stream.

It is clear from Fig. 3.1 that conversion increased with temperature. In the first stage of temperature range from 400 °C to 500 °C, the aromatics selectivity and yield increased with conversion, which is consistent with Andre's work in examining Pd contained catalyst [25]. The aromatics selectivity and yield are not proportional to the temperature as temperature went over 500 °C. The hydro-cracking process has been reinforced with increasing the temperature, which is reflected by the lower mass conversion, so that short chain alkanes were formed and evacuated with the carrier gas. This is contradictory to the assumption made by Kitagawa, et al. [26] in the study of transformation of propane into aromatics over ZSM-5 that demonstrated an increase in aromatics selectivity with temperature increased to 550 °C, in which short chain alkanes were used to build up into bigger molecular aromatics. At 600 °C, the chromatogram show high aromatic concentrations, while the mass yield was low due to the favored hydro-cracking. Consequently, the overall aromatics yield was unexpectedly lower than that at 500 °C.

The selectivity of all aromatics is shown in Fig. 3.2. Ethylbenzene and o-xylene were dominant among all the aromatics produced by the reaction, while m-xylene and p-xylene were present only in small amounts. This is consistent with Davis and Venuto's proposal of direct six-membered ring closure [27] that most of the aromatic products are formed by direct six-membered ring closure when heated greater than or equal to 480 °C. A possible explanation for the phenomena of similar selectivity to ethylbenzene and o-xylene, which also shown in the Pt/KL catalyzing n-octane dehydrocyclizaion, is that the length of the n-octane molecule is longer than the orifice on the Pd/C catalyst surface. It is only possible for the molecule to enter cavity and reach the active site lengthwise rather than transversely [28].

According to the molecular conformation, this orientation effect leads to the attachment of the  $\alpha$  or  $\beta$  carbon atom to the metal surface and the possibility of these two cases are almost equal. The similar results were also reported by Chevron workers [29-30] and Huang et al. [31] in their dehydrocyclization studies. For the formation of m-xylene and p-xylene, the n-octane molecule must go through isomerization reaction or five-membered ring intermediates [32], which are not promoted over Pd/C. Due to the geometric constraints of the pore channels, some of the C<sub>8</sub> aromatics may have to blunder along the channels, during which process the secondary reactions could occur. In the process, they may lose one or two carbon radicals to form benzene and toluene. In order to maximize C<sub>8</sub>-aromatics by avoiding secondary hydrogenolysis, zeolite with shorter pore length are required [33].

Conversion and total aromatics selectivity of n-octane dehydrocyclization at various WHSV has been reported in Table 3.1.

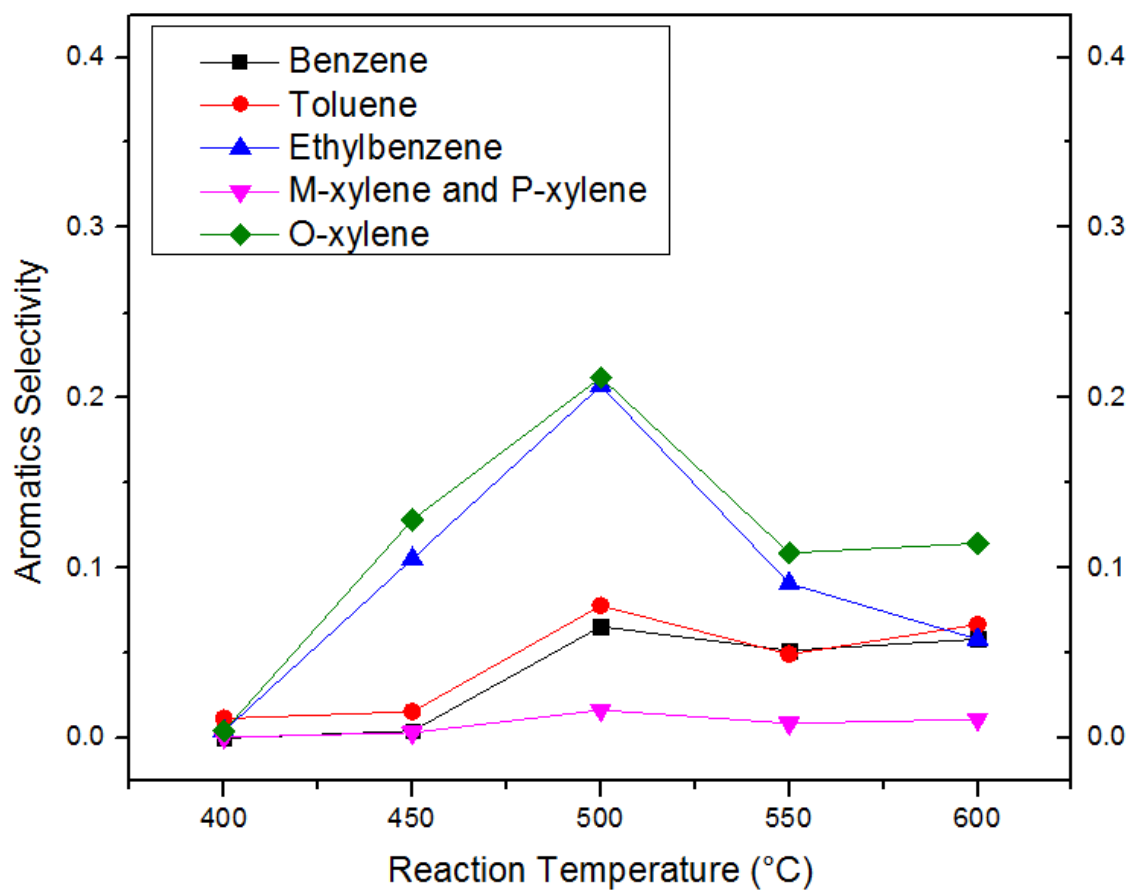


Figure 3.2 Effect of reaction temperature on aromatics selectivity during conversion of n-Octane over Pd/C

Reaction conditions: P=100 kPa, WHSV=2 h<sup>-1</sup>, H<sub>2</sub>/n-C8 molar ratio= 2, 30 min on stream.

Table 3.1 Conversion and total aromatics selectivity of n-octane dehydrocyclization over Pd/C at various WHSV

	WHSV*, h <sup>-1</sup>						
	0.8	1.0	2.0	4.0	8.0	16.0	Infinity
Conversion (%)	88.5	58.3	54.4	31.9	19.2	17.3	17.1
Aromatics selectivity (%)							
Benzene	9.6	3.8	6.6	2.0	0.5	0.2	0
Toluene	11.6	6.8	7.8	3.7	1.2	0.6	0
Ethylbenzene	12.6	22.0	20.7	14.7	8.0	4.8	0
m- and p-xylene	1.6	1.4	1.7	1.3	0.5	0.2	0
o-xylene	18.0	25.5	21.2	15.7	8.4	4.9	0
Aromatics yield (%)	47.2	34.7	31.5	11.9	3.6	1.8	0

Reaction conditions: P=100 kPa, T=500 °C, H<sub>2</sub>/n-C<sub>8</sub> molar ratio= 2, 30 min on stream.

\* The commercial Pd/C catalyst was originally wet; the catalyst was dried under low temperature in order to prevent oxidization, about 15% wt. moisture presence after drying.

The WHSV value was varied by varying the amount of catalyst tested in each run (Table 3.1). A noteworthy point is that though the conversion and aromatics yield increased with increasing the catalyst weight, the selectivity to ethylbenzene and o-xylene decreased when further adding catalyst to WHSV of  $0.8 \text{ h}^{-1}$ . These two aromatics are the product of direct six-membered ring closure, which is the primary reaction pathway. The excessive active sites of catalyst might have a poor desorption effect of these two aromatics because the reactant molecules can always find other sites to attach with. Another assumption is that the excessive active sites facilitate these two primary products of dehydrocyclization to be re-captured and further reacted. When no catalyst was loaded, i.e. WHSV to be infinity, there was 17.1% of conversion. However, no aromatics were made, and all the conversion was due to the high temperature hydro-cracking. This further verified that the catalyst was an indispensable aspect for dehydrocyclization to occur.

Table 3.2 Conversion and total aromatics selectivity of n-octane dehydrocyclization over Pd/C at various hydrogen/C8 molar ratios

	Hydrogen/n-C <sub>8</sub> molar ratio					
	0	0.5	1.0	2.0	3.0	6.0
Conversion (%)	50.0	52.9	52.2	54.4	50.9	61.6
Aromatics selectivity (%)						
Benzene	5.5	4.6	5.6	6.6	3.8	4.3
Toluene	6.8	5.4	6.9	7.8	4.4	6.0
Ethylbenzene	16.5	15.4	21.7	20.7	10.7	15.0
m- and p-xylene	1.6	1.4	1.8	1.7	0.9	0.2
o-xylene	19.3	17.4	23.1	21.2	11.1	15.4
Aromatics yield (%)	24.8	23.3	30.8	31.5	15.7	25.0

Reaction conditions: P=100 kPa, T=500 °C, WHSV=2 h<sup>-1</sup>, 30 min on stream.

Hydrogen to hydrocarbon molar ratio (MR) is known to be an important parameter that needs to be carefully controlled to balance the competing effects of, on the one hand, adequate hydrogen flowing is necessary to avoid catalyst deactivation; while on the other hand, dehydrocyclization is a process that produces hydrogen and is an equilibrium reaction favored by low hydrogen partial pressure. Also the excessive hydrogen promotes the hydrocracking pathway, which produced more small chain alkanes that were also the product of hydrogenation. Another important effect with the occurrence of the hydrogen is the generation of metal hydride. This reversible process is generally associated with a decrease in catalytic activity and sometimes is regarded as a poisoning process because the electronic structure of the parent metal has been disturbed [34]. There is some evidence to show that the Pd hydride could improve the hydrogenation of alkynes. Generally, there are both positive and negative effects, depending on the type of reaction desired and experimental conditions, of the hydride phase on the performance of Pd catalysts [35]; while the effect of Palladium hydride on aromatization has not been explored. Table 3.2 reveals the conversion, aromatics selectivity and yield with increasing hydrogen to hydrocarbon molar ratio. There is no specific trend of change with the variety of MR, which implies that the Pd hydride effect was trivial and negligible in this case. The better results appear in the middle range of the MR, which reasonably followed the pattern discussed above of hydrogen balance.

### 3.2 Comparisons between different catalysts

Table 3.3 shows the conversion, aromatics selectivity and aromatics yield of n-octane over Pd/C, Pt/C, Pd/Zeolite, Pt/KL, and Pt/Al<sub>2</sub>O<sub>3</sub>.

Table 3.3 Dehydrocyclization of n-octane over different Pd, Pt catalysts

catalyst	conversion (%)	Aromatics selectivity (%)					Aromatics Yield (%)
		Benzene	Toluene	Ethylbenzene	m- and p-xylene	o-xylene	
Pd/C	54.4	6.6	7.8	20.7	1.7	21.7	31.5
Pt/C	85.0	1.6	3.8	6.0	1.0	6.0	15.6
Pd/Zeolite	36.1	0	0.9	0	1.2	0.4	0.9
Pt/KL	74.5	22.2	4.3	0.8	0.3	0.7	21.1
Pt/ Al <sub>2</sub> O <sub>3</sub>	32.3	0.6	0.8	0.7	1.0	0.9	1.3

Reaction conditions: P=100 kPa, T=500 °C, WHSV=2 h<sup>-1</sup>, Hydrogen/n-C8 molar ratio=2, 30 min on stream.

The results of applying Pt/KL and Pt/ Al<sub>2</sub>O<sub>3</sub> for dehydrocyclization under the set experimental conditions (Table 3.3) were compared to those revealed from other references aforementioned. The conversion and selectivity of Pt/ Al<sub>2</sub>O<sub>3</sub> was unexpected considering the results of Rangel et al. [10] and Davis et al. [11]. The main reason might be related to the different structure of Al and procedure of synthesizing the catalyst, because alkane dehydrocyclization is generally considered as a structure sensitive reaction (i.e. its specific rates are dependent on particle size, single-crystal surface structure, or alloy composition.) [36]. Specifically for Pt/ Al<sub>2</sub>O<sub>3</sub> used in Rangel's study, 0.3% Pt was added on  $\gamma$  - Al<sub>2</sub>O<sub>3</sub> Ketjen CK300 35–80 mesh. Davis et al. used commercial UCI alumina. As for the performance of Pt/KL, the conversion in present study was consistent to that of Pt/KL (IWI) in Siriporn et al. work [15], while the aromatics selectivity was about half of that in his work. The different synthesizing process and reactor could be the cause of the deviation. The method of catalyst synthesis affects the distribution of the metal throughout the support and especially fraction of catalyst within the support pores.

From Table 3.3, Pd/C, Pt/C and Pt/KL were effective in catalyzing n-octane of hydrocyclization, therefore were chosen for longevity comparison. The deactivation curves of these catalysts as a function of reaction time are reflected by the diagrams below. The Pt contained catalysts showed higher conversion rate as well as a quick conversion decline compared to Pd/C. However, Pd/C featured a rapid drop on both aromatics selectivity and yield curve, though it had the highest initial aromatizing ability. In contrast, Pt/KL gave better stability with the aromatics selectivity and yield; Pt/C gave a smooth deactivation decline. Figure 3.4 was similar to the results of Pt/KL (IWI) reported by Siriporn et al. [15].

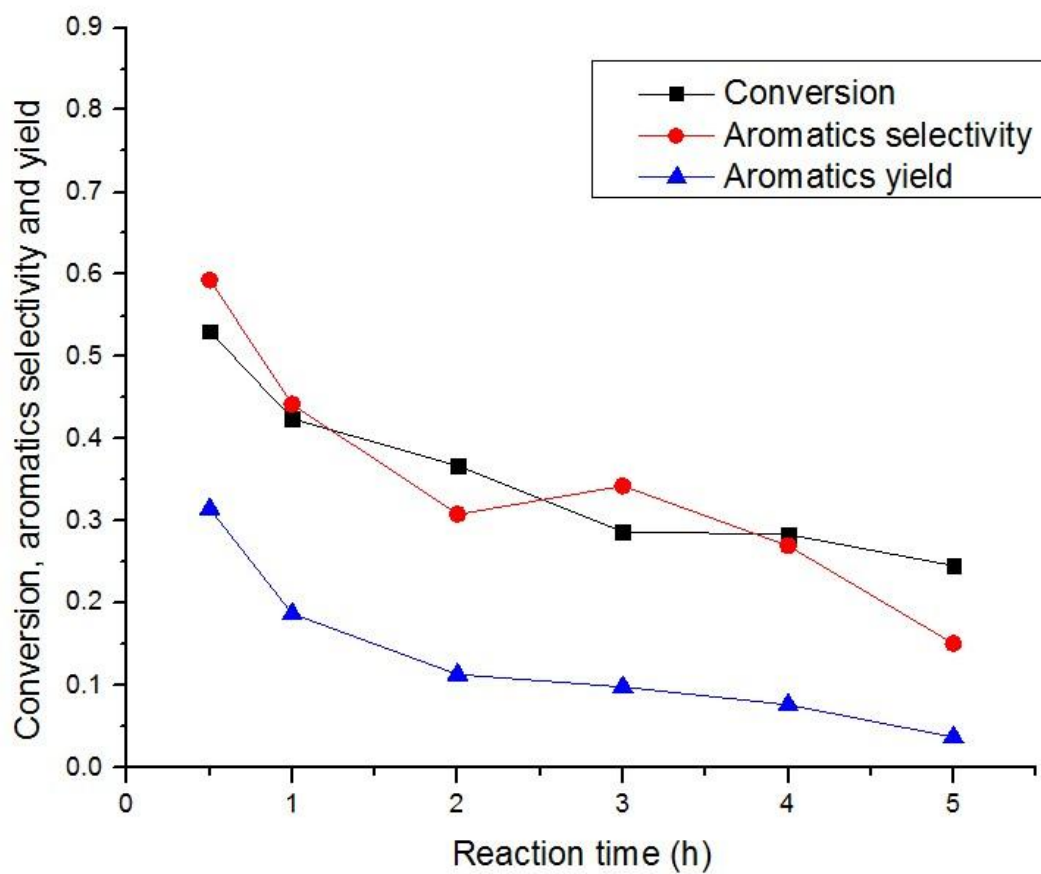


Figure 3.3 Effect of reaction time on total conversion, aromatics selectivity and yield of n-octane over Pd/C

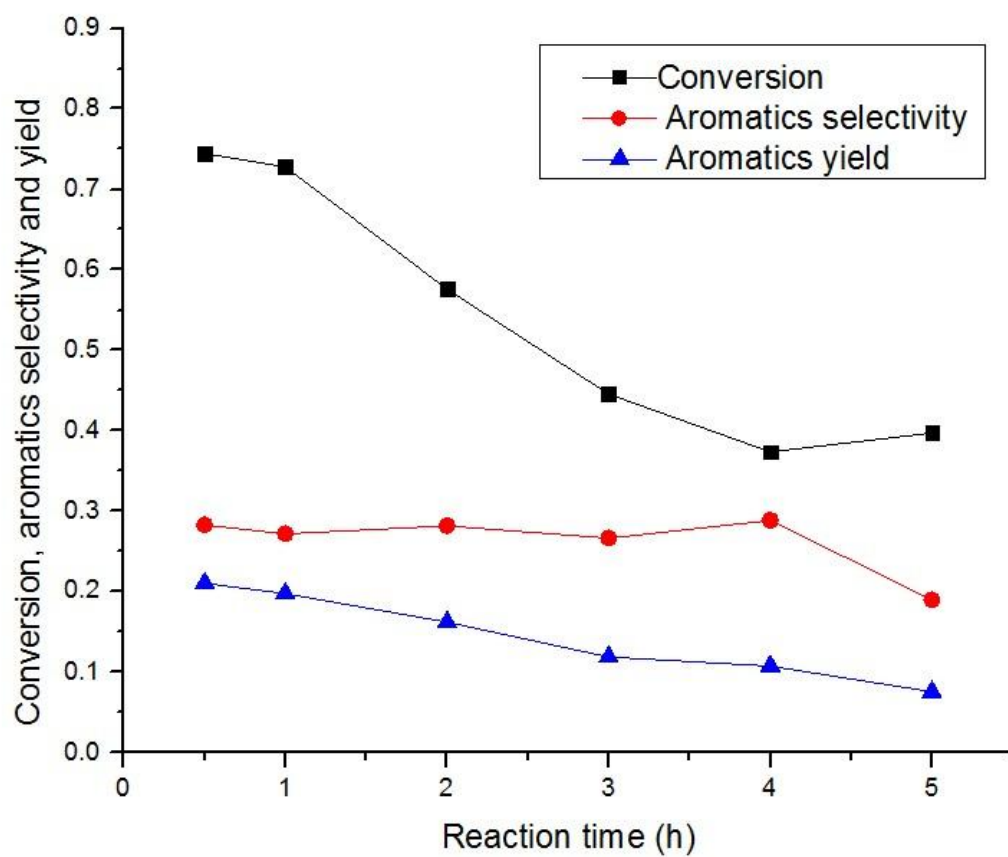


Figure 3.4 Effect of reaction time on total conversion, aromatics selectivity and yield of n-octane over Pt/KL

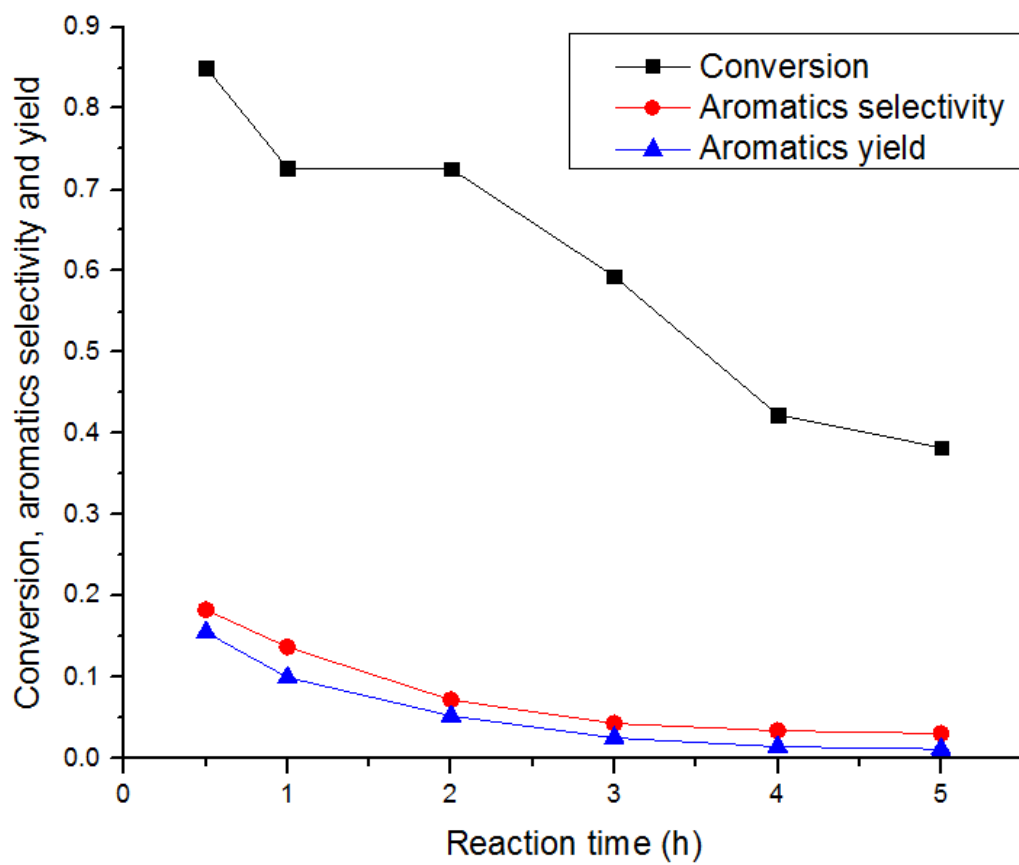


Figure 3.5 Effect of reaction time on total conversion, aromatics selectivity and yield of n-octane over Pt/C

The product distribution when tested with Pt/KL showed benzene and toluene as major aromatic products, with small quantities of ethylbenzene (EB) and o-xylene (OX), which are the only two expected products from a direct six-membered ring closure. The zeolite used in this study was the same product used by other researchers [33]. As they observed, the pore size of the KL zeolite is 0.71 nm, that is, larger than the critical diameter of EB but smaller than that of OX, thus OX diffuses through the zeolite crystal much more slowly than EB. As a result, OX is preferentially converted to benzene and toluene before escaping from the pore of zeolite. It was proposed that the pore length of the zeolite should have a great impact on product distribution and catalyst life [33]. Meanwhile the product distribution of Pd/C and Pt/C showed a similar mechanism, which is through direct six-membered ring closure. Since they were both supported on activated carbon, we could expect that the difference between these two catalysts was due to the different properties of Pd and Pt catalyzing aromatization.

It is postulated that the rate of deactivation should be much less pronounced at higher pressures, under conditions in which the presence of high partial pressures of hydrogen can help remove the coke precursors, and the catalyst activity is favored by 413~1379 kPa pressure, at which the adsorption process changes into a reversible process [22].

### 3.3 Comparisons between different feedstock

To investigate the selectivity of Pd/C in other hydrocarbons, exploratory experiments were conducted using n-hexane (Alfa Aesar, purity  $\geq 99\%$ ) and n-heptane (Alfa Aesar, purity  $\geq 99\%$ ) as reactants, separately. For each experiment, only the temperature of the vaporizer was changed to ensure that the reactant was vaporized completely in the vaporizer: n-hexane feeding, 100 °C; n-heptane feeding, 130 °C. Experiment conditions as follows: WHSV=2 h<sup>-1</sup>, hydrogen to n-alkane molar ratio=2, atmospheric pressure and reactor temperature=500 °C. Due to some inherent issues with the reactor setup, the mass conversion for these runs was very low. If taken into consideration for the calculation of conversion, aromatics selectivity and yield, the aromatics production would be very small. Therefore, only the identification of major products was conducted. Figure 6 shows the results of product (30 min on stream) provided by the GC/FID. For n-hexane as reactant, only benzene was produced, Fig. 3.6a. The GC/FID chromatogram showed high conversion, but the results cannot be quantitatively concluded with any certainty because a complete mass balance was not attempted for these exploratory experiments. For n-heptane as reactant, several aromatics were produced, Fig. 3.6b. These included benzene and toluene as well as one cycloalkane, methylcyclohexane. Figure 6c shows that from the aromatization of n-octane, benzene, toluene, ethylbenzene, m- and p-xylene, and o-xylene were produced.

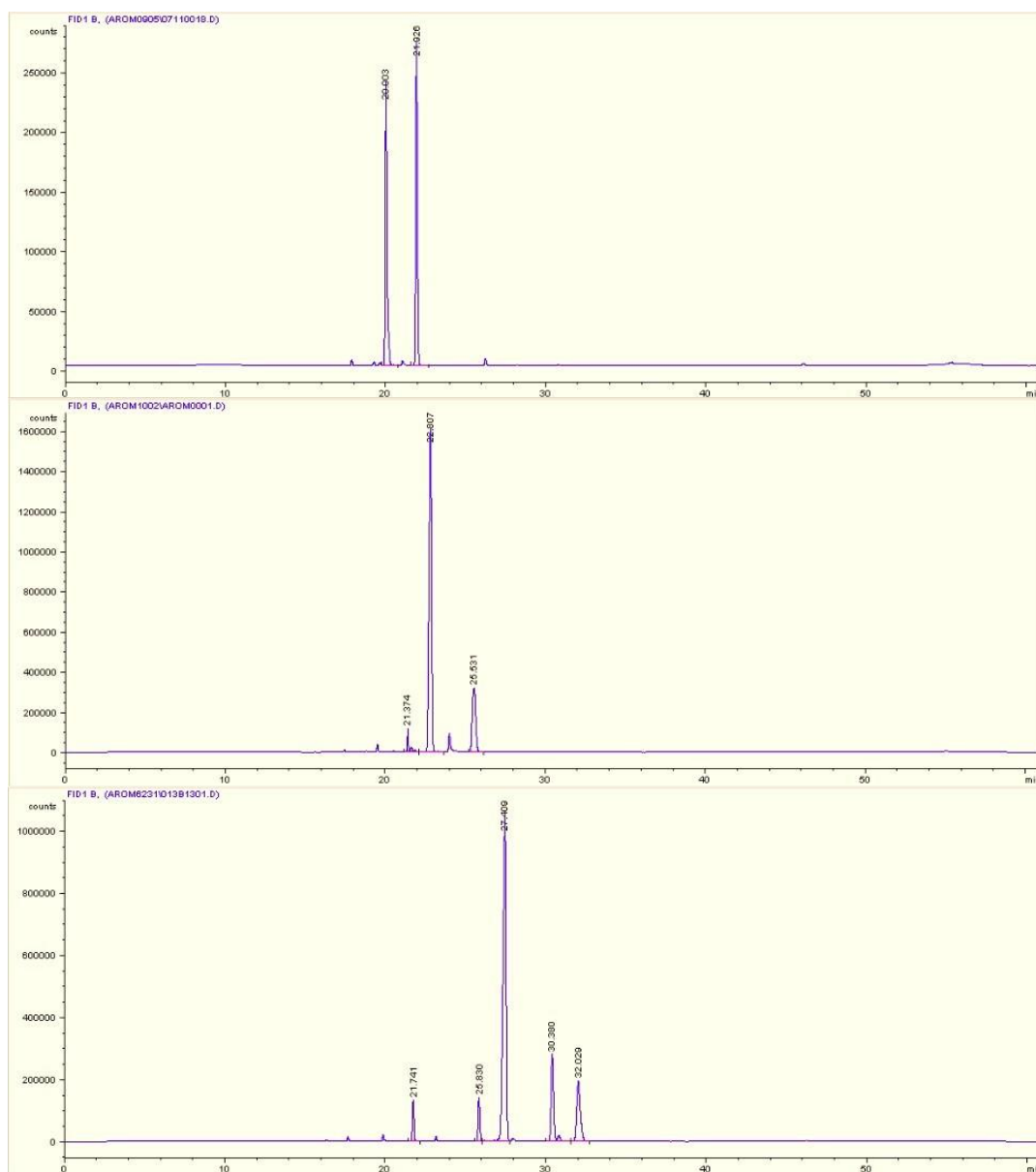


Figure 3.6 GC/FID chromatograms from aromatization over Pd/C of a) reactant: n-hexane (20 min), product: benzene (22 min); b) reactant: n-heptane (23 min), products: benzene (22 min), methylcyclohexane (24 min), toluene (25 min); c) reactant: n-octane (27 min), products: benzene (22 min), toluene (25 min), ethylbenzene (30 min), m- and p-xylene (31 min), o-xylene (33 min).

## Chapter 4 Conclusions

The Pd/C catalyst has seldom been reported for dehydrocyclization, but the present experiments indicated it is an effective catalyst for producing aromatics. It shows a high selectivity to alkylbenzenes rather than benzene as Pt/KL does. Ethylbenzene and o-xylene are two dominant aromatics in the product from n-octane aromatization under Pd/C catalysis. No aromatics were made with WHSV equaling infinity. Aromatics production was proportional to the catalyst amount. While with  $\text{WHSV} < 1$ , the excessive catalyst sites facilitates the secondary reactions to produce short chain aromatics. Aromatization is favored around 500 °C, and higher temperature promoted hydro-cracking. Hydrogen to hydrocarbon molar ratio is better kept around 2~3 in order to achieve a good aromatics yield.

Under the same experiment conditions, Pd/C had the highest initial catalytic efficiency compared to other Pt or Pd contained catalysts used in this work. Pt/KL showed better stability of aromatics selectivity. Pt contained catalysts featured high conversion as well as a rapid drop of conversion with time compared with Pd/C; while Pd/C showed a quicker aromatics selectivity decline than Pt contained catalysts.

The results of dehydrocyclization of n-octane over Pd/C greatly supported the six-membered ring closure that once the n-octane has been absorbed on the metal site, then two hydrogen atoms would be released and the paraffin would be cyclized to six-membered ring. The Pd/C is qualitatively capable of catalyzing n-alkanes of varying chain length. The reactants chosen here were surrogates for the complex streams of n-alkanes and iso-alkanes expected as reactants in the commercial configuration; hence future studies on evaluating

Pd/C with more complex reactant streams are needed. In addition, quantitative work on the conversion, aromatics selectivity and yield is recommended.

As pressure is important in retaining the activity of catalyst, pressurized dehydrocyclization should be done in the near future. Additionally, the kinetics of Pd/C needs to be explored before scaling-up.

## REFERENCES

- [1] DeWitt, Matthew J., et al. "Effects of Aromatic Type and Concentration in Fischer-Tropsch Fuel on Emissions Production and Material Compatibility." *Energy Fuels* 22.4 (2008; 2008): 2411-8.
- [2] Wargo J., Brown D., Cullen M., Addiss S. & Alderman N. *Children's Exposure to Diesel Exhaust on School Buses* Environmental and Human Health, Inc., North Haven, CT (2002).
- [3] EPA, Regulatory Announcement: Control of hazardous air pollutants from mobile sources: final rule to reduce mobile source air toxics, United States Environmental Protection Agency, Office of Transportation and Air Quality, EPA420-F-07-017, February 2007.
- [4] T. Edwards, L.Q. Maurice, Surrogate mixtures to represent complex aviation and rocket fuels, *Journal of Propulsion and Power* 2001 17(2) 461-466.
- [5] Yaws, Carl L. (2010). *Yaws' Thermophysical Properties of Chemicals and Hydrocarbons* (Electronic Edition). Knovel.  
Online version available at:  
[http://www.knovel.com/web/portal/browse/display?\\_EXT\\_KNOVEL\\_DISPLAY\\_bookid=2906&VerticalID=0](http://www.knovel.com/web/portal/browse/display?_EXT_KNOVEL_DISPLAY_bookid=2906&VerticalID=0)
- [6] Yaws, Carl L. (2003). *Yaws' Handbook of Thermodynamic and Physical Properties of Chemical Compounds*. Knovel. Online version available at:  
[http://www.knovel.com/web/portal/browse/display?\\_EXT\\_KNOVEL\\_DISPLAY\\_bookid=667&VerticalID=0](http://www.knovel.com/web/portal/browse/display?_EXT_KNOVEL_DISPLAY_bookid=667&VerticalID=0)

- [7] W.L. Roberts, H.H. Lamb, L.F. Stikeleather, T.L. Turner, inventors; North Carolina State University, assignee. Process for conversion of biomass to fuel. U.S. Patent No. 7,816,570. October 19, 2010.
- [8] M. Guisnet, N.S. Gnep, F. Alario. "Aromatization of Short Chain Alkanes on Zeolite Catalysts." *Applied Catalysis A: General* 89.1 (1992): 1-30.
- [9] Davis, Burtron H., and Paul B. Venuto. "Paraffin Dehydrocyclization: Distribution of Aromatic Products obtained with "nonacidic" Supported Pt Catalysts." *Journal of Catalysis* 15.4 (1969): 363-72.
- [10] Rangel, M. C., et al. "n-octane Reforming Over alumina-supported Pt, Pt-Sn and Pt-W Catalysts." *Catalysis Letters* 64.2 (2000): 171-8.
- [11] D.E. Sparks, R. Srinivasan, B.H. Davis, Paraffin dehydrocyclization. Part 8. Conversion of n-octane with mono and bifunctional Pt-Al<sub>2</sub>O<sub>3</sub> catalysts at 100 psig, *Journal of Molecular Catalysis* 88 (1994) 325-342.
- [12] Davis, Robert J., and Eric G. Derouane. "A Non-Porous Supported-Platinum Catalyst for Aromatization of n-Hexane." *Nature* 349.6307 (1991): 313-5.
- [13] Bernard, J. R. Proc. 5th int. Zeolite Conf. (ed. Rees, L. C. V.) 686-694 (Heyden, London, 1980).
- [14] Tamm, P. W., D. H. Mohr, and C. R. Wilson. "Octane Enhancement by Selective Reforming of Light Paraffins." *Studies in Surface Science and Catalysis. Volume 38 Vol. Elsevier* 335-353.
- [15] Jongpatiwut, Siriporn, et al. "N-Octane Aromatization on a Pt/KL Catalyst Prepared by Vapor-Phase Impregnation." *Journal of Catalysis* 218.1 (2003): 1-11.

- [16] Guisnet, M., N. S. Gnep, and F. Alario. "Aromatization of Short Chain Alkanes on Zeolite Catalysts." *Applied Catalysis A: General* 89.1 (1992): 1-30.
- [17] Iwasa, Nobuhiro, and Nobutsune Takezawa. "New Supported Pd and Pt Alloy Catalysts for Steam Reforming and Dehydrogenation of Methanol." *Topics in Catalysis* 22.3 (2003): 215-24.
- [18] Immer, Jeremy G., M. Jason Kelly, and H. Henry Lamb. "Catalytic Reaction Pathways in Liquid-Phase Deoxygenation of C18 Free Fatty Acids." *Applied Catalysis A: General* 375.1 (2010): 134-9.
- [19] Reetz, Manfred T., Rolf Breinbauer, and Klaus Wanninger. "Suzuki and Heck Reactions Catalyzed by Preformed Palladium Clusters and Palladiumnickel Bimetallic Clusters." *Tetrahedron letters* 37.26 (1996): 4499-502.
- [20] Franz n, Robert. "The Suzuki, the Heck, and the Stille Reaction - Three Versatile Methods for the Introduction of New C-C Bonds on Solid Support." *Canadian Journal of Chemistry* 78.7 (2000): 957-62.
- [21] Rom n-Mart nez, M. C., et al. "Metal-Support Interaction in Pt/C Catalysts. Influence of the Support Surface Chemistry and the Metal Precursor." *Carbon* 33.1 (1995): 3-13.
- [22] Burtron H., Davis. "Alkane Dehydrocyclization Mechanism." *Catalysis Today* 53.3 (1999): 443-516.
- [23] Agilent Technologies, National Institute of Standards and Technology 98 Mass Spectral Libraries, NIST 98, Rev. D.02.00, 2000.

- [24] Keith, Schofield. "The Enigmatic Mechanism of the Flame Ionization Detector: Its Overlooked Implications for Fossil Fuel Combustion Modeling." *Progress in Energy and Combustion Science* 34.3 (2008): 330-50.
- [25] Ramos, Andr e et al. "Reaction Pathway Studies of C6 Hydrocarbons on Palladium Model Catalysts: Effects of hydrogen/hydrocarbon Ratio, Molecular Structure, Surface Structure and Temperature." *Catalysis Letters* 66.1 (2000): 5-11.
- [26] Kitagawa, Hiroyoshi, Yoko Sendoda, and Yoshio Ono. "Transformation of Propane into Aromatic Hydrocarbons Over ZSM-5 Zeolites." *Journal of Catalysis* 101.1 (1986): 12-8.
- [27] Davis, Burtron H., and Paul B. Venuto. "Paraffin Dehydrocyclization: Distribution of Aromatic Products obtained with "nonacidic" Supported Pt Catalysts." *Journal of Catalysis* 15.4 (1969): 363-72.
- [28] Tauster, S. J., and J. J. Steger. "Molecular Die Catalysis: Hexane Aromatization Over Pt/KL." *Journal of Catalysis* 125.2 (1990): 387-9.
- [29] Hughes, T. R., Buss, W. C., Tamm, P. W., and Jacobson, R. L., in "Proceedings, 7th International Zeolite Conference" (Y. Murakami, A. Iijima, and J. W. Ward, Eds.), p. 725. Elsevier, Amsterdam, 1986.
- [30] Hughes, T. R., Jacobson, R. L., and Tamm, P. W., in "Catalysis 1987" (J. W. Ward, Ed.), pp. 317-333. Elsevier, Amsterdam, 1988.
- [31] Huang, Chen-Shi, et al. "Carbon-14 Tracer Study of the Conversion of Labeled n-Propylcyclopentane during n-Octane Aromatization with a Pt-Zeolite L Catalyst." *Journal of Catalysis* 134.1 (1992): 269-85.

- [32] Fling, Jingly, and Ikai Wang. "Dehydrocyclization of C6-C8 n-Paraffins to Aromatics Over TiO<sub>2</sub>-ZrO<sub>2</sub> Catalysts." *Journal of Catalysis* 130.2 (1991): 577-87.
- [33] Trakarnroek, Supak, et al. "Effect of Zeolite Crystallite Size on Pt/KL Catalysts used for the Aromatization of n-Octane." *Chemical Engineering Communications* 194.7 (2007).
- [34] Zolt n Pa , P. Govind Menon. *Hydrogen Effects in Catalysis: Fundamental and Practical Applications*. CRC Press, 1988.
- [35] Nag, Nabin K. "A Study on the Formation of Palladium Hydride in a Carbon-Supported Palladium Catalyst." *The Journal of Physical Chemistry B* 105.25 (2001; 2001): 5945-9.
- [36] Gillespie, W. D., et al. "The Structure Sensitivity of n-Heptane Dehydrocyclization and Hydrogenolysis Catalyzed by Platinum Single Crystals at Atmospheric Pressure." *Journal of Catalysis* 70.1 (1981): 147-59.